"Symmetry and symmetry breaking in nuclear physics"
17th Nuclear Physics Workshop, "Marie & Pierre Curie"
22-26th, September 2010, Kazimierz

Configuration mixing of angular-momentum projected triaxial relativistic mean-field wave functions

Jiangming Yao (尧江明)

西南大学物理科学与技术学院
School of Physical Science and Technology,
Southwest University, Chongqing, China

25th, September, 2010

Outline

Low-lying states of exotic nuclei

- Radioactive nuclear beam facilities and gamma ray detectors have in recent years allowed one to study spectroscopy of the low-lying excited states for exotic nuclei. It provides rich information about the nuclear structure, including

Low-lying states of exotic nuclei

- Radioactive nuclear beam facilities and gamma ray detectors have in recent years allowed one to study spectroscopy of the low-lying excited states for exotic nuclei. It provides rich information about the nuclear structure, including
  1. evolution of shell structure and collectivity

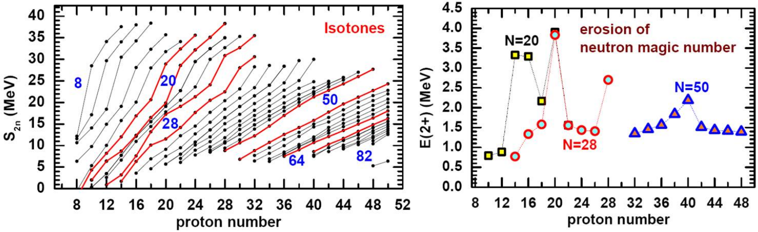

  2. nuclear shape and shape phase transition

     R. F. Casten, Nature Physics, 811 (2006); P. Cejnar, Rev. Mod. Phys. 82, 2155 (2010)
  3. decoupling of neutrons and protons (in ^{16}C)

     N. Imai et al., Phys. Rev. Lett. 92, 062501 (2004)

Beyond the SC mean-field approach for nuclear low-lying states

In the past decade, several beyond SC mean-field models have been developed that perform the restoration of symmetries broken by the static nuclear mean field, and take into account fluctuations around the mean-field minimum.

Restricted to axial shape

- PNP+1DAMP+GCM (HF with Skyrme force)
  A. Valor, P.-H. Heenen, and P. Bonche, NPA671, 145(2000)
- PNP+1DAMP+GCM (HFB with Gogny force)
  R. Rodriguez-Guzman, J. L. Egido, and L. M. Robledo, NPA709, 201(2002)
- PNP+1DAMP+GCM (RMF with point-coupling force)
  T. Niksic, D. Vretenar, and P. Ring, PRC73, 034308 (2006)

Beyond the SC mean-field approach for nuclear low-lying states

In the past decade, several beyond SC mean-field models have been developed that perform the restoration of symmetries broken by the static nuclear mean field, and take into account fluctuations around the mean-field minimum.

Restricted to axial shape

- PNP+1DAMP+GCM (HF with Skyrme force)
  A. Valor, P.-H. Heenen, and P. Bonche, NPA671, 145(2000)
- PNP+1DAMP+GCM (HFB with Gogny force)
  R. Rodriguez-Guzman, J. L. Egido, and L. M. Robledo, NPA709, 201(2002)
- PNP+1DAMP+GCM (RMF with point-coupling force)
  T. Niksic, D. Vretenar, and P. Ring, PRC73, 034308 (2006)

Applications for nuclear low-lying states

- low-spin normal-deformed and super-deformed collective states
  Bender, Flocard & Heenen, PRC68, 044321 (2003)
- shape coexistence in Kr, Pb isotopes
  Rodriguez-Guzman, Egido & Robledo, PRC 69, 054319 (2004);
  Bender, Bonche & Heenen, PRC 74, 024312 (2006)
- shell closures at N=32 or 34?
  Rodriguez & Egido, PRL 99, 062501 (2007)
- shape transition in Nd isotopes
  Niksic, Vretenar, Lalazissis & Ring, PRL99, 092502 (2007);
  Rodriguez & Egido, PLB 663, 49 (2008)

Beyond the self-consistent mean-field theory: Recent progress

Recently, the 1DAMP+GCM framework has been extended to the 3DAMP+GCM case, which makes it possible to study the nuclear low-lying states with the consideration of effects from

1. restoration of rotation symmetry in full 3D Euler space
2. shape fluctuation in full β-γ plane

Non-relativistic versions

- PNP+3DAMP+GCM (HFB with Skyrme force)
  M. Bender and P.-H. Heenen, PRC78, 024309 (2008).
- PNP+3DAMP+GCM (HFB with Gogny force)
  T. R. Rodriguez and J. L. Egido, Phys. Rev. C 81, 064323 (2010)

Only illustrative calculations have been carried out in non-relativistic frameworks !

Beyond the self-consistent mean-field theory: Recent progress

Recently, the 1DAMP+GCM framework has been extended to the 3DAMP+GCM case, which makes it possible to study the nuclear low-lying states with the consideration of effects from

1. restoration of rotation symmetry in full 3D Euler space
2. shape fluctuation in full β-γ plane

Non-relativistic versions

- PNP+3DAMP+GCM (HFB with Skyrme force)
  M. Bender and P.-H. Heenen, PRC78, 024309 (2008).
- PNP+3DAMP+GCM (HFB with Gogny force)
  T. R. Rodriguez and J. L. Egido, Phys. Rev. C 81, 064323 (2010)

Only illustrative calculations have been carried out in non-relativistic frameworks !

Our relativistic 3DAMP+GCM model

starting from the RMF+BCS with point-coupling force
Yao, Meng, Ring & Pena Arteaga, PRC79, 044312 (2009);
Yao, Meng, Ring & Vretenar, PRC81, 044311 (2010)

1. framework of our relativistic 3DAMP+GCM model
2. its applications to the analysis of nuclear low-lying states in some interesting isotopes.

Outline

Intrinsic states from the relativistic point-coupling calculations

The relativistic 3DAMP+GCM model

1. The relativistic point-coupling model+BCS calculations with constraints on quadrupole moments by minimizing the energy functional

$$E'[\rho_i, j_i^\mu] = E[\rho_i, j_i^\mu] - \sum_{\mu=0,2} \frac{C_\mu}{2}(\hat{Q}_{2\mu} - q_{2\mu})^2 \quad (1)$$

generate a large set of highly correlated intrinsic deformed states $|\Phi(q)\rangle$. The pairing correlations, for open-shell nuclei, are taken into account by augmenting the following pairing energy functional,

$$E[\kappa] = -\sum_\tau \int d\mathbf{r} \frac{V_\tau}{4} \kappa_\tau^*(\mathbf{r})\kappa_\tau(\mathbf{r}) \quad (2)$$

with separately adjustable strengths $V_{p/n}$ for protons and neutrons.

PC-F1: Burvenich, Madland, Maruhn & Reinhard, PRC65, 044308 (2002).
DD-PC1: Niksic, Vretenar & Ring, PRC78, 034318 (2008).
PC-PK1: Zhao, Li, Yao & Meng, arXiv:1002.1789v1 [nucl-th].

Configuration of angular momentum projected triaxial states

The relativistic 3DAMP+GCM model

2. The nuclear wavefunction with good angular momentum and shape fluctuation is obtained by projecting the intrinsic states $|\Phi(\beta,\gamma)\rangle$ onto good angular momentum (K-mixing) and performing GCM calculations (configuration mixing),

$$|\Psi_\alpha^{JM}\rangle = \int d\beta d\gamma \sum_{K\geq 0} f_\alpha^{JK}(\beta,\gamma) \underbrace{\frac{1}{(1+\delta_{K0})}[\hat{P}^J_{MK} + (-1)^J \hat{P}^J_{M-K}]}\, |\Phi(\beta,\gamma)\rangle \tag{3}$$

The weight functions f_α^{JK} are determined from the solution of Hill-Wheeler-Griffin (HWG) integral equation: $q \equiv (\beta,\gamma)$

$$\int dq' \sum_{K'\geq 0} \left[\mathscr{H}^J_{KK'}(q,q') - E^J_\alpha \mathscr{N}^J_{KK'}(q,q')\right] f_\alpha^{JK'}(q') = 0, \tag{4}$$

where $\mathscr{H}$ and $\mathscr{N}$ are the angular-momentum projected GCM kernel matrices of the Hamiltonian and the Norm, respectively.

Electromagnetic moments and transition strengths

The relativistic 3DAMP+GCM model

3. The electromagnetic moments and transition strengths are evaluated with the nuclear wavefunction.

- $E0$ and $E2$ transition strengths
- g-factor: $\mu(J^\pi)/J$
- Spectroscopic quadrupole moment: $Q^{\rm spec}(J)$
- $\cdots$

$$B(\sigma\lambda; J_i, \alpha_i \to J_f, \alpha_f) = \frac{e^2}{2J_i+1} \sum_{M_i \mu M_f} \left| \langle J_f, M_f, \alpha_f | \hat{M}(\sigma\lambda\mu) | J_i, M_i, \alpha_i \rangle \right|^2 \quad (5)$$

The matrix elements are calculated in the full configuration space. There is no need for effective charges.

Outline

1. Introduction
   - Low-lying states of exotic nuclei
   - Beyond the self-consistent mean-field theory
2. The relativistic 3DAMP+GCM model
3. **Application for nuclear low-lying states**
   - A well deformed nucleus Dysprosium
   - Magnesium isotopes
   - Carbon isotopes
4. Summary and perspective

Low-lying states in ^{166}Dysprosium: AMP

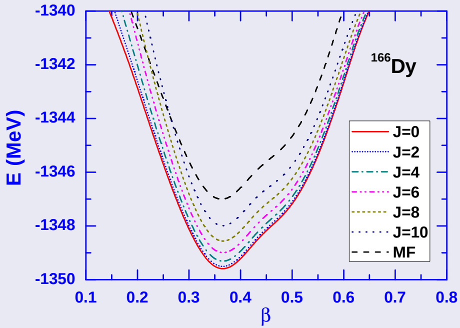

- A pronounced minimum with $\beta = 0.350$ in the mean-field potential energy surface.
- After angular momentum projection, one obtains the projected PES with $J = 0, \cdots, 10$.
- The projected PES with $J = 0$ has a minimum with $\beta = 0.375$.
- The energy gained from AMP is about 3 MeV.

Low-lying states in ^{166}Dysprosium: comparison with a rigid rotor

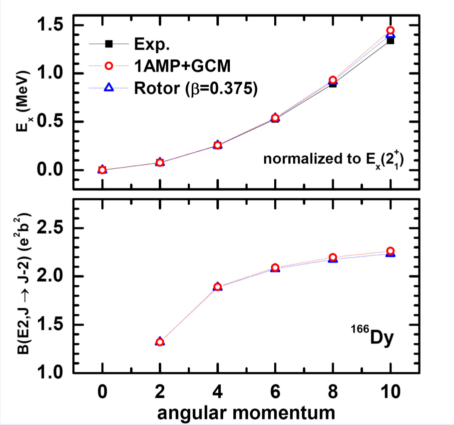

Figure: The excitation energies [normalized to $E_x(2_1^+)$] and $B(E2)$ values of low-lying states as functions of angular momentum.

- Good agreement has been found between the rigid rotor model and microscopic projected GCM calculations, both of which reproduce the data quite well.

Low-lying states in magnesium isotopes: correlation energies

Total dynamical correlation energies $E_{\rm Corr}$ consists of two parts:

1. energy correction from the restoration of rotational symmetry

$$\Delta E_{J=0} = E_{J=0}(\beta_0) - E_{\rm MF}(\beta_m), \tag{6}$$

2. the energy correlation from configuration mixing

$$\Delta E_{\rm GCM} = E(0_1^+) - E_{J=0}(\beta_0). \tag{7}$$

Low-lying states in magnesium isotopes: correlation energies

Total dynamical correlation energies $E_{\rm Corr}$ consists of two parts:

1. energy correction from the restoration of rotational symmetry

$$\Delta E_{J=0} = E_{J=0}(\beta_0) - E_{\rm MF}(\beta_m), \tag{6}$$

2. the energy correlation from configuration mixing

$$\Delta E_{\rm GCM} = E(0_1^+) - E_{J=0}(\beta_0). \tag{7}$$

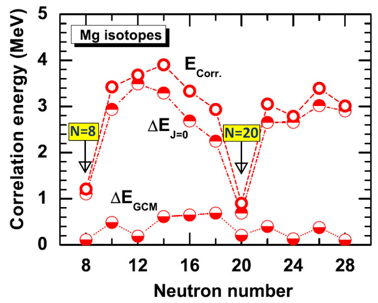

Figure: Total ground-state dynamical correlation energies of Mg isotopes, as a function of the number of neutrons.

- $E_{\rm Corr}$ shows a strong dependence on shape and shell structure.
- large for deformed mid-shell nuclei, with a maximum of ~ 4 MeV at $N = 14$, and is drastically reduced (~ 1 MeV) for the two isotopes with the neutron magic numbers $N = 8$ and $N = 20$.
- The rotational energy correction $\Delta E_{J=0}$ constitutes the dominant part.

Non-Rel. Cal.+GOA: Bender, Bertsch & Heenen, PRC73, 034322 (2006).

Low-lying states in magnesium isotopes: E2 transition strengths

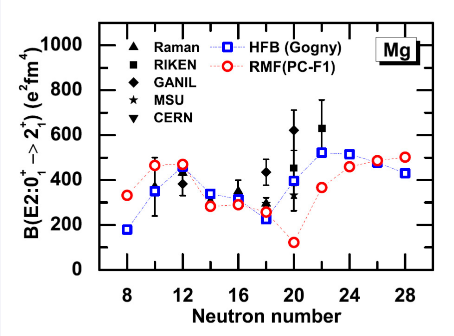

Figure: $B(E2; 0_1^+ \rightarrow 2_1^+)$ (e^2fm^4) values in $^{20-40}$Mg, calculated using the 1DAMP+GCM model with the relativistic density functional PC-F1, are compared to available data and the results of the 1DAMP+GCM calculation based on the non-relativistic HFB framework with the Gogny force [*Rodriguez-Guzman, Egido & Robledo, NPA709, 201 (2002)*].

- Our calculations (PC-F1) yield results in reasonable agreement with data except, of course, at and in the neighborhood of the neutron number $N = 20$.
- A better adjustment of pairing strength parameters and eventually the inclusion of triaxiality, could improve the results for ^{32}Mg, giving $B(E2; 0_1^+ \rightarrow 2_1^+) = 330.1$ e^2fm^4, much closer to the available data.

Effect of triaxiality in E0 transition of ^{30}Mg

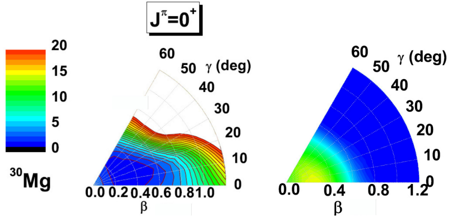

The projected PES ($J = 0$) and Probability distribution of 0_1^+ state in β-γ plane.

Table: Results from 1D and 3DAMP+GCM calculations with the relativistic PC-F1 force and non-relativistic Gogny force, compared to experimental values. Both the non-relativistic calculation results and experimental data are taken from Ref.[*W. Schwerdtfeger et al., PRL 103, 012501 (2009)*].

	$E_x(2_1^+)$ (MeV)	$E_x(0_2^+)$ (MeV)	$\rho_{21}^2(E0)\times 10^3$	$B(E2;0_1^+\to 2_1^+)$ (e^2fm^4)	$B(E2;0_2^+\to 2_1^+)$ (e^2fm^4)
Exp.	1.482	1.789	26.2±7.5	241(31)	53(6)
3D(PC-F1)	1.713	2.864	24.72	277	68↑
1D(PC-F1)	1.905	3.275	15.56↓	257	47
1D(Gogny-D1S)	2.03	2.11	46 ↑	334.6	181.5↑

Excitation energies and BE2 values in Carbon isotopes

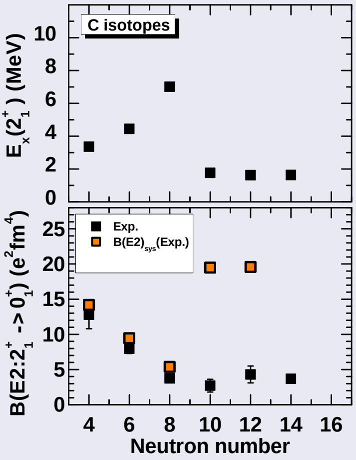

Figure: Excitation energies of 2_1^+ states $E_x(2_1^+)$ (MeV) and the $B(E2)$ values (e^2fm^4) for even-even carbon isotopes.

- The experiment $B(E2)$ values are compared with the prediction by the empirical relation: *S. Raman et al., PRC37, 805 (1988)*

$$\begin{aligned} & B(E2: 0_1^+ \to 2_1^+)_{\mathrm{sys.}} \\ = \quad & 6.47 Z^2 A^{-0.69} E_x^{-1}(2_1^+). \end{aligned} \qquad (8)$$

Excitation energies and BE2 values in Carbon isotopes

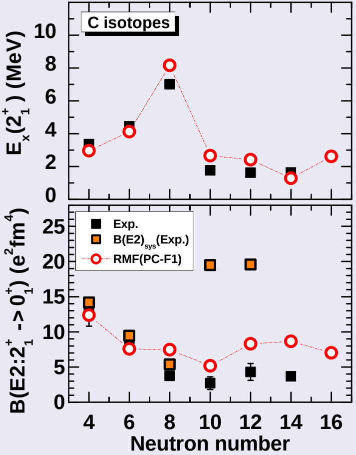

Figure: Excitation energies of 2^+_1 states $E_x(2^+_1)$ (MeV) and the $B(E2)$ values (e^2fm^4) for even-even carbon isotopes.

- The experiment $B(E2)$ values are compared with the prediction by the empirical relation: *S. Raman et al., PRC37, 805 (1988)*

$$B(E2:0^+_1\to 2^+_1)_{\text{sys.}} = 6.47 Z^2 A^{-0.69} E_x^{-1}(2^+_1). \tag{8}$$

- The systematics of both $E_x(2^+_1)$ and $B(E2:2^+_1\to 0^+_1)$ are reproduced quite well
- The quenched $B(E2)$ values, combined with the very low $E_x(2^+_1)$ indicate that the decoupled structure of neutron and proton exist in $^{16-20}$C.

Excitation energies and BE2 values in Carbon isotopes

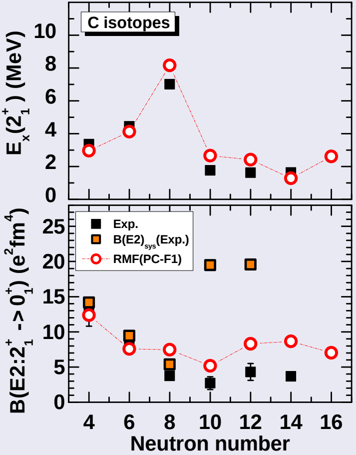

Figure: Excitation energies of 2_1^+ states $E_x(2_1^+)$ (MeV) and the $B(E2)$ values (e^2fm^4) for even-even carbon isotopes.

- The experiment $B(E2)$ values are compared with the prediction by the empirical relation: *S. Raman et al., PRC37, 805 (1988)*

$$B(E2:0_1^+ \to 2_1^+)_{\text{sys.}} = 6.47 Z^2 A^{-0.69} E_x^{-1}(2_1^+). \qquad (8)$$

- The systematics of both $E_x(2_1^+)$ and $B(E2:2_1^+ \to 0_1^+)$ are reproduced quite well
- The quenched $B(E2)$ values, combined with the very low $E_x(2_1^+)$ indicate that the decoupled structure of neutron and proton exist in $^{16-20}$C.
- The large difference between neutron and proton deformations in $^{16-20}$C is due to the special mp-2h configurations $\nu(1d_{5/2})^m \otimes \pi(1p_{3/2})^{-2}$, $m = 2, 4, 6$.

Excitation energies and BE2 values in Carbon isotopes

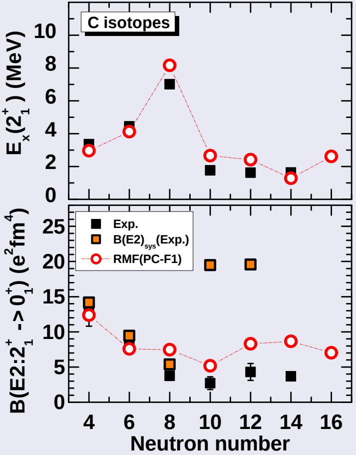

Figure: Excitation energies of 2_1^+ states $E_x(2_1^+)$ (MeV) and the $B(E2)$ values (e^2fm^4) for even-even carbon isotopes.

- The experiment $B(E2)$ values are compared with the prediction by the empirical relation: *S. Raman et al., PRC37, 805 (1988)*

$$
\begin{aligned}
& B(E2:0_1^+ \to 2_1^+)_{\mathrm{sys.}} \\
= \quad & 6.47 Z^2 A^{-0.69} E_x^{-1}(2_1^+).
\end{aligned} \tag{8}
$$

- The systematics of both $E_x(2_1^+)$ and $B(E2:2_1^+ \to 0_1^+)$ are reproduced quite well
- The quenched $B(E2)$ values, combined with the very low $E_x(2_1^+)$ indicate that the decoupled structure of neutron and proton exist in $^{16-20}$C.
- The large difference between neutron and proton deformations in $^{16-20}$C is due to the special mp-2h configurations $\nu(1d_{5/2})^m \otimes \pi(1p_{3/2})^{-2}$, $m = 2, 4, 6$.
- What about ^{22}C? Neutron halo with $\nu(2s_{1/2})^2$? *K. Tanaka et al., PRL 104, 062701 (2010)*

Outline

Summary

The relativistic version of 3DAMP+GCM approach and its applications

- The relativistic 3DAMP+GCM model has been developed that uses the generator coordinate method (GCM) to perform configuration mixing of three-dimensional angular-momentum projected (3DAMP) relativistic mean-field wave functions, generated by constrained self-consistent calculations for triaxial nuclear shapes.
- The relativistic 3DAMP+GCM model has been tested and compared with the rigid rotor model for the low-spin states in well deformed nucleus ^{166}Dy.
- The low-lying states of magnesium isotopes and carbon isotopes have been calculated. The spectroscopic properties, including excitation energy, $BE0$, $BE2$ transition strengthes and g-factor, are studied. The effects of triaxiality and pair correlation are discussed.
- Triaxiality has been found to be important in ^{30}Mg.
- The quenched $B(E2)$ values, combined with the very low $E_x(2_1^+)$ indicate that the decoupled structure of neutron and proton exist in $^{16-20}$C.

Perspective

What can be done next?

- Using a separable pairing force in the pairing channel.
  Tian, Ma & Ring, PLB676, 44 (2009).
- Comparing with the same energy functional based Bohr Hamiltonian calculation to examine the Gaussian Overlap Approximation.
  Niksic, Li, Vretenar, Prochniak, Meng & Meng, PRC79, 034303 (2009)
- Including two quasiparticle configurations using the idea of projected shell model.
  Hara & Sun, Int. J. Mod. Phys. E 4, 637-785 (1995)
- Augmenting the particle number projection and regularization
  Lacroix, Duguet & Bender, PRC79, 044318 (2009).
  Bender, Duguet & Lacroix, PRC79, 044319 (2009).
- . . .

Acknowledgments

To my collaborators

Jie Meng	Peking Univ.
Zhipan Li	Southwest Univ. China
Peter Ring, Daniel Pena Arteaga	TUM
Dario Vretenar	Zagreb Univ.
Kouichi Hagino	Tohoku Univ.

Thanks for Your attention!

Numerical details

- **Imposed symmetries:** parity, D_2 symmetry, and time reversal symmetry.
- **Basis expansion method:** a set of three-dimensional isotropic harmonic oscillator basis functions in Cartesian coordinates.
- **Modified Broyden's method** for accelerating convergence in self-consistent calculations *A. Baran et al., PRC 78, 014318 (2008)*
- The **Gaussian-Legendre quadrature** is used for integrals over the Euler angles ϕ, θ and ψ in the calculation of the norm and hamiltonian kernels.

Low-lying states in magnesium isotopes: g-factor

- g-factor: $g(J^\pi_\alpha) = \mu(J^\pi_\alpha)/J$, where the magnetic moment $\mu(J^\pi_\alpha)$ of excited state J^π_α can be calculated with the angular momentum projected wave function,

$$\mu(J^\pi_\alpha) \quad = \quad \langle J, M = J, \alpha | \hat{\mu}_{10} | J, M = J, \alpha \rangle \tag{9}$$

The magnetic moment vector $\hat{\mu}$ is related to effective electromagnetic current operator,

$$\hat{\mu}_k = \frac{1}{2} \int d^3 r [\mathbf{r} \times \mathbf{j}]_k, \;\; k = x, y, z \tag{10}$$

that is determined by the effective EM current,

$$\hat{\mathbf{j}} = e\psi^\dagger \alpha \psi + \frac{\kappa}{2M} \nabla \times [\psi^\dagger \beta \mathbf{\Sigma} \psi], \tag{11}$$

where κ is the free anomalous gyromagnetic ratio of the nucleon: $\kappa^p = 1.793$ and $\kappa^n = -1.913$.

Low-lying states in magnesium isotopes: g-factor

- g-factor: $g(J^\pi_\alpha) = \mu(J^\pi_\alpha)/J$, where the magnetic moment $\mu(J^\pi_\alpha)$ of excited state J^π_α can be calculated with the angular momentum projected wave function,

$$\mu(J^\pi_\alpha) \quad = \quad \langle J, M = J, \alpha | \hat{\mu}_{10} | J, M = J, \alpha \rangle \qquad (9)$$

The magnetic moment vector $\hat{\mu}$ is related to effective electromagnetic current operator,

$$\hat{\mu}_k = \frac{1}{2} \int d^3r [\mathbf{r} \times \mathbf{j}]_k, \;\; k = x, y, z \qquad (10)$$

that is determined by the effective EM current,

$$\hat{\mathbf{j}} = e\psi^\dagger \alpha \psi + \frac{\kappa}{2M} \nabla \times [\psi^\dagger \beta \mathbf{\Sigma} \psi], \qquad (11)$$

where κ is the free anomalous gyromagnetic ratio of the nucleon: $\kappa^p = 1.793$ and $\kappa^n = -1.913$.

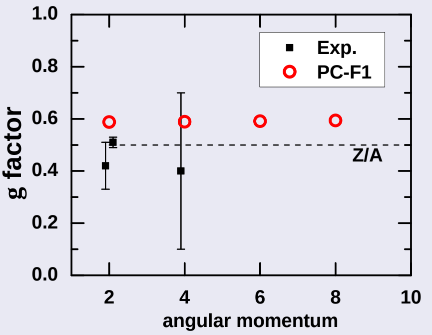

Figure: The g-factor as a function of angular momentum in ^{24}Mg.

Potential energy curves in Carbon isotopes

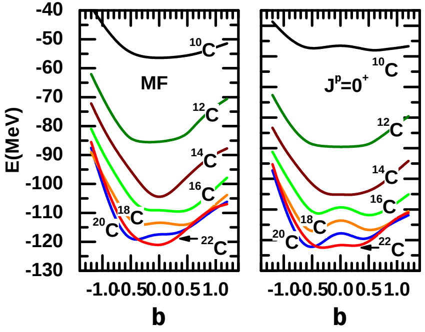

Figure: Self-consistent RMF+BCS mean-field (left panel), and angular-momentum projected 0^+ potential energy curves (right panel) of even-even magnesium isotopes, as functions of the axial deformation parameter β.

Potential energy curves in Carbon isotopes

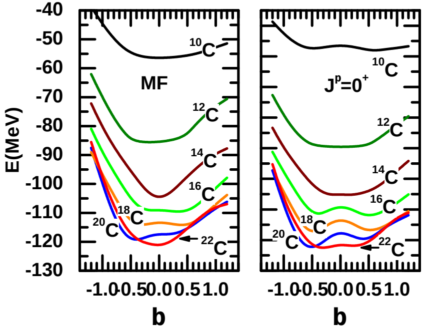

Figure: Self-consistent RMF+BCS mean-field (left panel), and angular-momentum projected 0^+ potential energy curves (right panel) of even-even magnesium isotopes, as functions of the axial deformation parameter β.

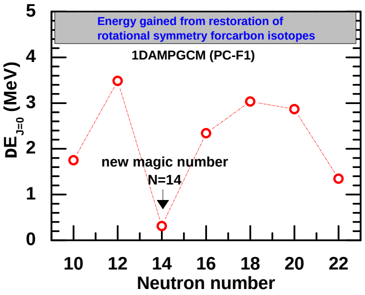

Figure: The rotational energy correction $\Delta E_{J=0}$ as a function of neutron number.

$$\Delta E_{J=0} = E_{J=0}(\beta_0) - E_{\rm MF}(\beta_m), \quad (12)$$

where β_m and β_0 denote the axial deformation parameters at the minima of the mean-field and the $(J^\pi = 0^+)$ angular-momentum projected PECs, respectively

probability

The solution of HWG equation determines both the energies E_α^J and the amplitudes $f_\alpha^{JK}(q)$ of collective states with good angular momentum $|\Psi_\alpha^{JM}\rangle$

$$f_\alpha^{JK}(q) = \sum_k \frac{g_k^{J\alpha}}{\sqrt{n_k^J}} u_k^J(i). \tag{13}$$

The weight functions $f_\alpha^{JK}(q)$ are not orthogonal and cannot be interpreted as collective wave functions for the deformation variables. The collective wave functions $g_\alpha^J(i)$ are calculated from the norm overlap eigenstates:

$$g_\alpha^J(i) = \sum_k g_k^{J\alpha} u_k^J(i), \tag{14}$$

The wave functions $g_\alpha^J(i)$ are orthonormal and, therefore, $|g_\alpha^J(i)|^2$ can be interpreted as a probability amplitude.